Fuel 390 (2025) 134738

Contents lists available at ScienceDirect

Fuel

journal homepage: www.elsevier.com/locate/fuel

Full Length Article

Revealing the aging mechanisms of solketal, oxymethylene ether, and mixtures thereof as promising e-fuels

Anne Lichtinger [a], Maximilian J. Poller [a], Olaf Schröder [b], Julian Türck [c,d], Thomas Garbe [e], Jürgen Krahl [f,g], Markus Jakob [b], Jakob Albert [a,*]

[a] University of Hamburg, Institute of Technical and Macromolecular Chemistry, Bundesstrasse 45, 20146 Hamburg, Germany
[b] Coburg University of Applied Sciences and Arts, Friedrich-Streib-Strasse 2, 96450 Coburg, Germany
[c] Leuphana University, Universitaetsallee 1, 21335 Lueneburg, Germany
[d] TECOSOL GmbH, Jahnstrasse 2, 97199 Ochsenfurt, Germany
[e] Volkswagen AG, Berliner Ring 2, 38440 Wolfsburg, Germany
[f] OWL University of Applied Sciences and Arts, Campusallee 12, 32657 Lemgo, Germany
[g] FUELS JOINT RESEARCH GROUP, www.fuels-jrg.de, Germany

ARTICLE INFO

Keywords:
E-fuels
Solketal
OME
Fuel mixtures
Aging mechanism

ABSTRACT

Solketal and oxymethylene ether (OME) are two promising blending candidates for regenerative fuels (e-fuels), which could contribute to a holistic solution to the energy crisis. In this study the thermo-oxidative aging of these two e-fuels in their pure form as well as in binary mixtures with different ratios (3:1, 1:1, and 1:3) (vol%) is investigated. Herein, the reaction networks of the thermo-oxidative aging process of both e-fuels and mixtures thereof is elucidated based on intermediates and decomposition products determined via GC–MS. Furthermore, changes of important fuel-specific parameters like kinematic viscosity and density as well as total acid number during aging have been determined. The 3:1 solketal:OME (vol%) mixture exhibits a higher stability to thermo-oxidative aging than the pure fuel components or mixtures with other ratios. The viscosity value of this mixture is within the DIN EN 590 norm after accelerated aging of 72 h (viscosity (72 h) = 4.25 mm^2/s)) unlike other blends. The maximum value of the total acid number of this aged mixture reaches only ~ 29 % of the maximum value of aged pure OME and has the lowest value of all mixtures. Furthermore, the formation of a precipitate could be successfully suppressed in the 3:1 solketal:OME (vol%) mixture different from other mixtures. With these findings, this study contributes to the design of new sustainable fuels for the transport sector.

1. Introduction

In order to achieve climate neutrality in the EU by 2050, CO_2 emissions must be reduced drastically [1]. As 25 % of the total greenhouse gas emissions in the EU come from the transport sector [1], defossilization of the latter is essential to achieve the climate protection goals. Defossilization can be achieved by switching to renewable energy sources and using renewable fuels such as biofuels or e-fuels [2]. As a beneficial side-effect, this also helps to reduce the dependence on oil and gas exporting countries, which is of great importance given the current political situation in eastern Europe.

The production of biodiesel, a biofuel consisting of fatty acid methyl esters has been established for several years [3], whereby large amounts of glycerol as a by-product are produced. The crude glycerol produced by the biodiesel industry (70 % purity) contains impurities such as water, inorganic salts, methanol, fatty acids and esters [4] and therefore cannot be used in the food or cosmetics industry. Glycerol has a high boiling point (290 °C) and a high viscosity (1.412 Pa s at room temperature), in addition it has a corrosive effect and acrolein is emitted during combustion [3]. Therefore, it cannot be used as a pure fuel or as a blend component. However, by ketalization with acetone, which can be produced from biomass, e.g., through the acetone-butanol-ethanol (ABE) fermentation process [5], glycerol can be used for the production of solketal (isopropylidene glycerol). Solketal is a promising substance to be used as a regenerative fuel (biofuel) component [4,6,7] (Fig. 1). The acid catalyzed [4,8,9] condensation reaction of glycerol and acetone can lead to the formation of five-membered and six-membered rings (ketals) [4,10,11], but the five-membered ketal is

---

* Corresponding author.
E-mail address: jakob.albert@uni-hamburg.de (J. Albert).

https://doi.org/10.1016/j.fuel.2025.134738
Received 18 September 2024; Received in revised form 5 February 2025; Accepted 13 February 2025

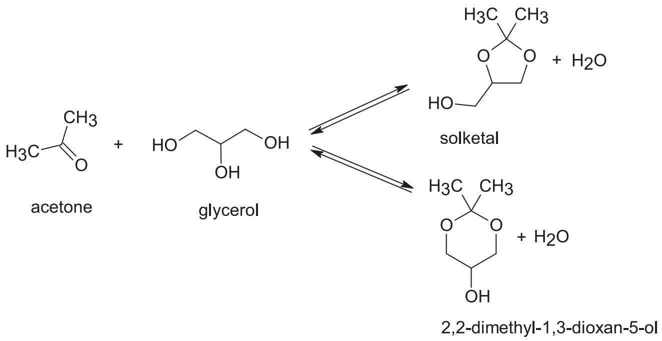

Fig. 1. Formation of solketal: condensation reaction of acetone and glycerol to solketal (five-membered ring) or 2,2-dimethyl-1,3-dioxan-5-ol (six-membered ring) [4].

highly favored with a ratio of 99:1 [4,12,13].

Solketal has a higher oxygen content compared to fossil fuels, which means less chemical energy can be stored and released during combustion. This is expressed by a lower specific heating value [3,14]. However, the lower number of C–C bonds and the absence of double bonds in the solketal molecule also leads to reduced soot formation during combustion, and thereby lower particle emissions [3]. The use of solketal as a fuel additive has shown these effects alongside and improved cold flow properties [4,15]. Furthermore, when added to gasoline, gum formation is reduced and the octane number is increased [4,16].

OME are oxymethylene ethers, i.e., acetals with the chemical structure $CH_3[OCH_2]_nOCH_3$. The chain length n determines the physical properties of the OME. OME_1 to OME_5 are liquid, from OME_6 onwards the oxymethylene ethers are solid [17,18]. OME is similar in structure to the polymer POM (polyoxymethylene), which, however, has a much higher degree of polymerization (chain length $\geq$ 2000) compared to OME [17,19,20]. There are several synthetic pathways for the production of OME. OME_1 (dimethoxy methane) is commonly synthesized from methanol and formaldehyde. Long-chain OME_n are formed by reacting OME_1 with trioxane, which is obtained from formaldehyde in the pressure swing process [18,21–23]. An alternative synthesis route describes the direct synthesis of OME via methanol and formaldehyde, without trioxane as an intermediate [18,24] (Fig. 2). Methanol is commonly produced from fossil-based syngas (CO/H_2) [18], but can also be synthesized sustainably from green H_2 and CO_2[25]. Formaldehyde can be obtained from methanol by silver catalyzed oxidation [18,26].

$OME_{3\text{-}5}$ are non-toxic and have similar physical properties as fossil diesel fuel [17,18]. However, they show a strong potential for reducing soot formation during combustion, as there are no direct C–C bonds in the OME molecules [17,18,27]. This largely resolves the conflict of optimizing combustion temperatures to either avoid NO_x (lower temperatures desired) or reduce soot emissions (higher temperatures desired) [18]. This allows operation of the engine with low NO_x and low particulate emissions at the same time (through exhaust gas recirculation). There have been several studies regarding the pyrolysis of OME. De Ras et al. [28] investigated the pyrolysis of OME_2 over a broad temperature range and found a decomposition of OME_2 to formaldehyde and OME_1 at temperatures below 800 K. In addition to unimolecular decomposition, radicals and intermediate products like methane, methyl formate and formaldehyde were formed at higher temperatures.

Solketal as a biofuel component and OME as an e-fuel are both promising regenerative fuels due to their advantageous characteristics. However, some of the fuel parameters of their pure form do not fulfill the fuel standard DIN EN590 [29], e.g., the viscosity of solketal is too high, while it is too low for OME. But it is important for using a fuel that its characteristics are within the norm. Therefore, some mixtures of both have to be found which are in the desired range to get regenerative fuels that can directly be used as fuels or fuel components, with promising fuel properties.

Blends of gasoline or diesel fuel with solketal as well as blends of diesel fuel with OME were already investigated [3,6,16,30]. But mixtures of solketal and OME have been, to the best of our knowledge, only studied very little so far. These mixtures can also be blended with diesel fuel or FAME (fatty acid methyl esters) to form a ternary mixture that could be used as fuel, similar to Diesel R33 [31].

If fuels are stored for a longer period of time, for example as emergency energy storage or in the case of hybrid vehicles, fuel aging is a major concern [2]. The aging of conventional fossil fuels and biodiesel through autoxidation is a phenomenon that has been known for many years and is widely discussed in the literature, for example by Pradelle et al. [32], Rizwanul Fattah et al. [33] and others [32–39]. However, further aging studies are essential for the use of new, regenerative fuels. Cychy et al. [40] and Kumari et al. [41] have carried out electro-oxidative studies on solketal using electrocatalysts for synthetic purposes. They found, in addition to the main product glyceric acid, some other products, like glyceraldehyde and oxalic acid [40,41]. Moity et al. [42] investigated cyclic glycerol acetals and ketals as bio-based solvents and their stability with regard to pH-value dependent hydrolysis. They also investigated the oxidation of these compounds with the PetroOxy device [43] up to 4 h. They found that neither acetals nor ketals are stable in an acidic media but acetals exhibited a higher stability than ketals. Furthermore, they found that formaldehyde and acetone acetals

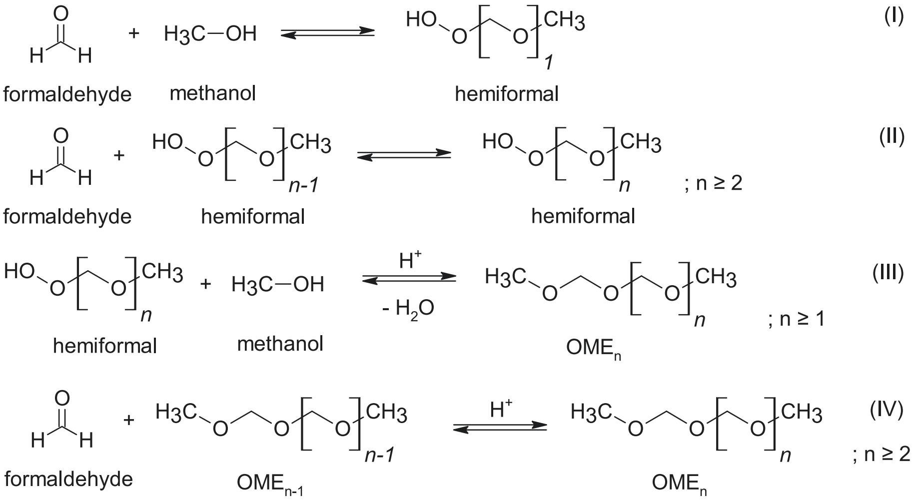

Fig. 2. Synthesis process of oxymethylene ether (OME_n): synthesis to OME_n from methanol and formaldehyde [24].

Table 1

Fuel specific parameters (extract) of solketal and oxymethylene ether (OME). 100-S: pure solketal, 100-O: pure OME, mixtures of 3:1 (75-S-25-O), 1:1 (50-S-50-O) and 1:3 (25-S-75-O) solketal:OME (vol%).

parameter	100-S	100-O	75-S-25-O	50-S-50-O	25-S-75-O	DIN EN 590
boiling range [°C]	188–189 [7]	156–242 [17] (OME $_{3\text{-}5}$)				180 – 390 [17]
flashpoint [°C]	85 [16]	54–115 [17] (OME $_{3\text{-}5}$)				>55 [17]
kin. viscosity (T = 40 °C) [mm^2/s]	5.02	1.21	3.05	2.02	1.51	2.00–4.50 [17]
density (T = 15 °C) [kg/m^3]	1.07	1.06	1.07	1.06	1.06	0.820–0.845 [17]

are very stable against autoxidation, whereas glycerol-based ketals are more stable than ethylene glycol-based ketals [42]. Türck et al. [3,6,44] have investigated the influence of solketal on the aging of biodiesel (by blending with C18:1 as a model fuel or by blending with biodiesel/diesel mixtures). They have discovered that the addition of solketal has an influence on the aging of biodiesel, for example changes in viscosity or total acid number [3,44].

The degradation of polyoxymethylene was investigated in the 1960 s and early 1970 s. It was found that the most important degradation mechanism is oxidative, whereas thermal decomposition occurs via chain reactions of free radicals at temperatures between 100 °C-170 °C [20,45–48]. However, it is not clear to what extent the aging of polyoxymethylene is transferable to the aging of OME, as the influence of the chain length was not investigated. Bogatykh et al. [20] investigated OME aging with the aid of the Rancimat method. The authors identified various degradation products and investigated the induction time of an OME-mix ($OME_{3\text{-}5}$) as a function of different concentrations of the added antioxidant BHT (butyl hydroxy toluene). Furthermore, the influence of hydroperoxides on the induction time was investigated. They found that hydroperoxides have a detrimental effect and BHT led to a higher oxidation stability of OME [20].

The here presented study, in contrast to earlier work, investigates in detail the time-dependent concentrations of the individual OME_1 – OME_6 and the different aging products of the solketal-aging. Furthermore, the exact reaction pathways are elucidated in order to get a better understanding of the formation of the various aging products. Also, the time-dependent changes in important fuel-specific parameters, such as the kinematic viscosity, density and total acid number of different mixtures of solketal and OME and the influence of solketal on OME-aging and vice versa are deduced.

2. Experimental

2.1. Fuels and chemicals

All chemicals were used as received without further purification. Solketal with a purity ≥ 97 % was purchased from Sigma Aldrich. OME (unadditivated) was purchased from ASG (product number 2803710_001). The composition of OME can vary considerably from batch to batch. According to the data sheet, the composition of the OME used in this research is: 0.05 wt% OME_1, 0.06 wt% OME_2, 45.39 wt% OME_3, 5.11 wt% OME_3-derivative, 25.39 wt% OME_4, 2.23 wt% OME_4-derivative, 11.22 wt% OME_5 and 4.57 wt% OME_6[49]. The OME-derivatives are shown in the supporting information (Fig. S1). The chemicals for calibration and the pure paraformaldehyde (chain length $n = 8$–100) were purchased from Carl Roth and Sigma Aldrich. The different OME_n in pure form for calibration were kindly provided from ASG.

2.2. Experimental setup and working procedure of fuel aging

For the accelerated thermo-oxidative aging of the fuels, the aging setup described in detail in previous articles [2,50] was used (Figure S2, section 1). The fuel was aged in a three-neck round bottom flask, which was placed in an oil bath (T = 110 °C). To minimize the release of volatile aging products, a Dimroth reflux condenser (T = 2 °C) was positioned above the flask. To oxidize the fuel, dry air was introduced into the fuel at a constant flow rate of 10 l/h via a gas introduction tube. These conditions were based on the Rancimat method (according to DIN EN 14112 [51] and DIN EN 15751 [52]). This aging setup was operated as an open aging system. The air introduced into the fuel was directed through the reflux condenser into a wash bottle containing deionized water. At the start of the aging process, the flask contained 250 ml of the fuel to be aged. To monitor the aging products over time, a 25 mL fuel sample was taken from the flask every 24 h. For this purpose, the stopper of the flask was briefly opened and 25 ml of the aged fuel was removed using a glass pipette. The samples were subsequently analyzed with GC–MS of FT-IR spectroscopy (vide infra). The fuel was aged for a total of 144 h. For a more detailed description, see references [2,50].

2.3. Analytical methods

An Agilent GC7890A gas chromatograph coupled to an Agilent 5973 quadrupole mass spectrometer was used for the gas chromatography with coupled mass spectrometry (GC–MS) measurements. It was equipped with a Phenomenex Zebron ZB-5 HT column with a length of 30 m, an inner diameter of 0.25 mm and a pathlength of 0.25 µm. The carrier gas was helium with a flow rate of 35.5 mL/min. 2 µl of the sample was injected and the split ratio was 20:1. In the temperature program, the oven was held at 80 °C for 10 min, then brought to 120 °C at 3 °C/min. After a holding time of 2 min, the oven was brought to 250 °C at 5 °C/min and then to 300 °C at 15 °C/min. The spectra were compared with the NIST08 database for product identification. To determine the concentration of the aging products, a calibration series was performed with each of the pure substances and an internal standard. The determination of the concentration of OME_2 is described in the supporting information (section 2). For the aging products that were not available in pure form, the peaks of the products were integrated and the areas of the products were divided by the peak areas of the internal standard (peak area $_{\text{analyte}}$ / peak area $_{\text{internal standard}}$).

The Fourier transformed infrared (FT-IR) spectroscopy measurements were carried out using a Thermo Scientific Nicolet 6700 FTIR spectrometer with a diamond ATR unit (attenuated total reflectance). The single bounce ATR unit has a wavelength cutoff of 650 cm^{-1} through a ZnSe lens and an angle of incidence of 42°. The penetration depth of the 1.5 mm diamond is 2.03 µm at 1000 cm-1. The spectrometer has a DTGS detector (deuterated triglycine sulphate) and an XT–KBrTM beam splitter (extended KBr range) [2,50].

The kinematic viscosity and the density were assessed using a Stabinger viscosimeter from Anton Paar. To carry out the measurements, 3

Table 2
Products of the thermo-oxidative aging of solketal.

component	aging time
solketal + 2,2-dimethyl-1,3-dioxan-5-ol	0 h – 144 h
glycerol	24 h – 144 h
acetone	24 h – 144 h
2,2-dimethyl-1,3-dioxolane-4-carboxaldehyde	24 h – 144 h
glyceraldehyde	24 h – 144 h
acetic acid	24 h – 144 h
2,2-dimethyl-1,3-dioxolane-4-carboxylate	24 h – 144 h
2,2-dimethyl-1,3-dioxolane-4-methanol-acetate	24 h – 144 h
2,2-dimethyl-1,3-dioxolane	24 h – 144 h
acetine (2,3-dihydroxypropyl acetate)	48 h – 144 h
hydroxy acetic acid	96 h – 144 h
(1,3-dioxolane-4-yl)methanol + 1,3-dioxane-5-ol	96 h – 144 h
methyl hydroxy acetate	96 h – 144 h

ml of the sample was injected into the device using a syringe. The viscosity measurements were carried out at a temperature of 40 °C and the density measurements at a temperature of 15 °C. The data processing of the measurements was done with the Rheoplus software from Anton Paar [2,50].

The total acid number (TAN) was determined using the potentiometric titration method in accordance with DIN EN 12634. An 888 Titrando and an 801 stirrer, both from Metrohm, were used to carry out these measurements. A glass electrode suitable for non-aqueous media was used for the titration. The measuring solution consisted of potassium hydroxide dissolved in 2-propanol (0.1 mol/L). The solvent used for the analysis consisted of 50 vol% toluene, 49.5 vol% 2 - propanol and 0.5 vol% deionized water, with a total volume of 60 mL per sample. The sample weight varied depending on the expected total acid number and ranged from 0.505 g to 10.007 g. The TAN is the amount of base, expressed in milligrams of potassium hydroxide per gram of fuel (mg KOH/g), required to neutralize the acids present in the sample.

3. Results and discussion

In order to compare OME, solketal and mixtures thereof with conventional diesel fuel, the fuel properties according to the fuel standard DIN EN 590 were assessed first. The fuel properties of OME and solketal correspond to those of diesel fuel in terms of boiling range and flash point (Table 1). The kinematic viscosity of solketal is 5.02 mm^2/s, that of OME is 1.21 mm^2/s. According to DIN EN 590, the kinematic viscosity for a diesel fuel must be 2.00–4.50 mm^2/s [17]. Mixtures with ratios of 1:1 and 3:1 (solketal:OME) (vol%) are within the desired range and were consequently used in this study. In detail, the aging of mixtures of 3:1 (75-S-25-O), 1:1 (50-S-50-O) and 1:3 (25-S-75-O) solketal:OME (vol%) in addition to pure solketal (100-S) and pure OME (100-O) were investigated.

In order to understand the aging of solketal and OME as well as their mixtures, the thermo-oxidative aging process of these fuels was accelerated using a previously established setup [2,50] (Figure S2) to apply 110 °C and a flow of 10*L*/h dry air. During this process, samples were taken every 24 h and analyzed by GC–MS or, in case of a solid-state aging product, by FT-IR. Additionally, the fuel specific parameters viscosity, density, and TAN have been determined.

3.1. Thermo-oxidative aging of solketal

The initial sample of solketal already contained some of its isomer, 2,2-dimethyl-1,3-dioxan-5-ol, but no glycerol or acetone were detected.

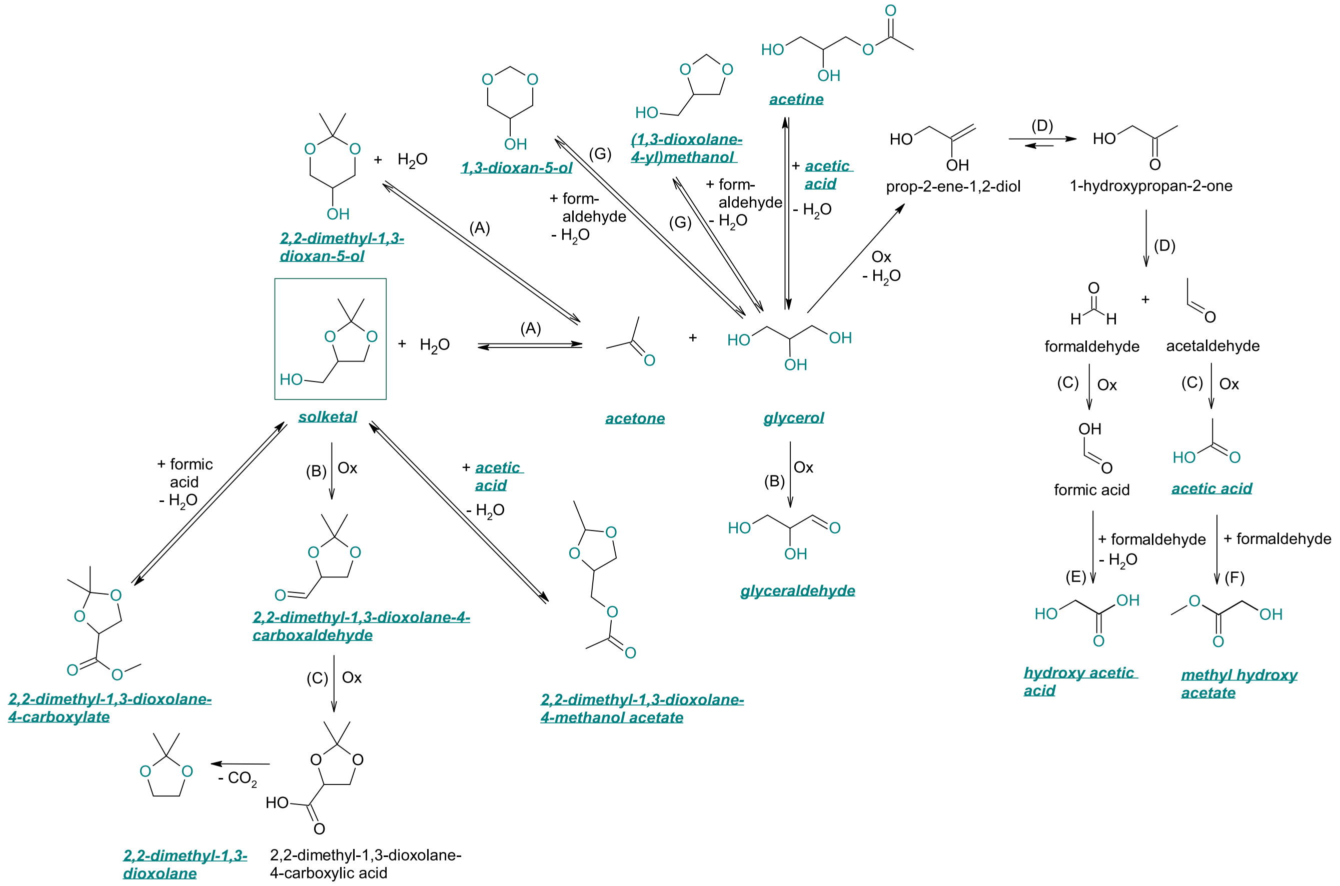

Fig. 3. Reaction pathway of the thermo-oxidative aging of solketal, the compounds detected by GC–MS are highlighted. References used: (A): [4]; (B): [50,53,54]; (C): [50,54,55]; (D): [56–58]; (E): [60]; (F): [59]; G: [61].

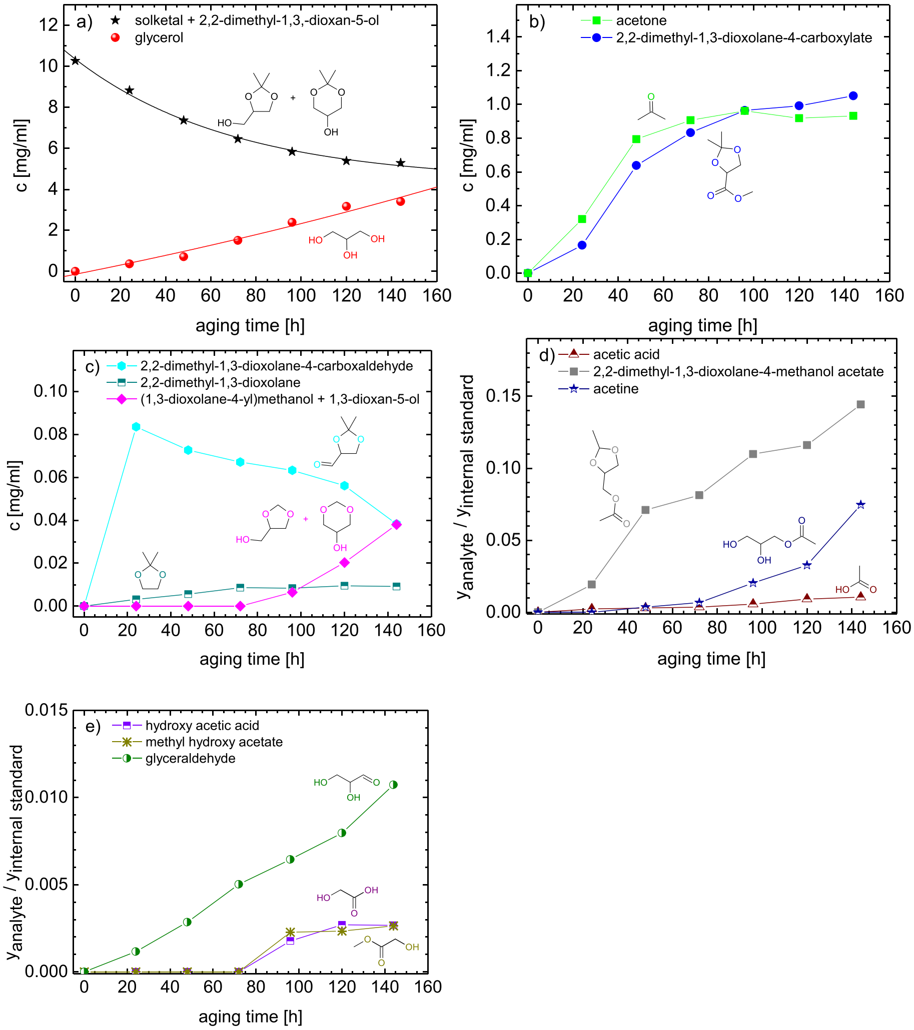

Fig. 4. a, b, c) Time course of the concentrations of various products of the thermo-oxidative aging of solketal. d, e) Normalized peak area as a function of the aging time of various products of the thermo-oxidative aging of solketal.

Table 3
Components of the thermo-oxidative aging of OME.

component	aging time
OME_1	0 h – 144 h
OME_2	0 h – 144 h
OME_3	0 h – 144 h
OME_4	0 h – 144 h
OME_5	0 h – 144 h
OME_6	0 h – 144 h
formic acid	24 h – 144 h
methyl formate	24 h – 144 h
hydroxy acetic acid	48 h – 144 h
methyl hydroxy acetate	48 h – 144 h
paraformaldehyde	72 h – 144 h

Starting from the 24 h sample, glycerol and acetone were found, next to glyceraldehyde, acetic acid, 2,2-dimethyl-1,3-dioxolane and some of its derivatives. After 48 h, acetine (2,3-dihydroxypropyl acetate) was found, and after 96 h hydroxy acetic acid, (1,3-dioxolan-4-yl)methanol and 1,3-dioxan-5-ol, as well as methyl hydroxy acetate could also be detected (Table 2).

Based on the observed products and known reaction pathways from other studies [4,50,53–61], the following reaction pathway for the aging of solketal is postulated (Fig. 3):

During thermo-oxidative aging, hydrolysis of the ketalization of solketal occurs from an aging time of 24 h, resulting in the two products glycerol and acetone. Alternatively, solketal can be oxidized directly via autoxidation [50,53,54] to form aldehyde 2,2-dimethyl-1,3-dioxolane-4-carboxaldehyde, which can then be further oxidized to 2,2-dimethyl-1,3-dioxolane-4-carboxylic acid (solketalic acid) by autoxidation [50,54,55]. Although the acid could not be detected, its formation is inferred by the observation of 2,2-dimethyl-1,3-dioxolane, which results from its decarboxylation. The glycerol resulting from hydrolysis of solketal can similarly be oxidized to glyceraldehyde by autoxidation [50,53,54]. Furthermore, glycerol can also form 1-hydroxypropan-2-one via oxidative C–C bond cleavage, which itself can react further to produce formaldehyde and acetaldehyde [56–58].

Both of these aldehydes subsequently oxidized to their corresponding acids, formic acid and acetic acid [50,54,55], which are inferred because of the detection of hydroxy acetic acid and methyl hydroxy acetate. Their formation can be explained by a reaction of the aforementioned acids with formaldehyde [59,60]. Similarly, a reaction of formaldehyde with glycerol explains the observation of (1,3-dioxolane-4-yl)methanol [61]. Analogous to the synthesis of solketal (Fig. 1), both the five-membered ring (1,3-dioxolane-4-yl)methanol and the six-membered ring 1,3-dioxan-5-ol can be formed [61].

Moreover, glycerol can be esterified with acetic acid to form acetine (2,3-dihydroxypropyl acetate). Furthermore, a reaction of formic acid with solketal yields 2,2-dimethyl-1,3-dioxolane-4-carboxylate, and similarly the esterification of solketal with acetic acid produces 2,2-

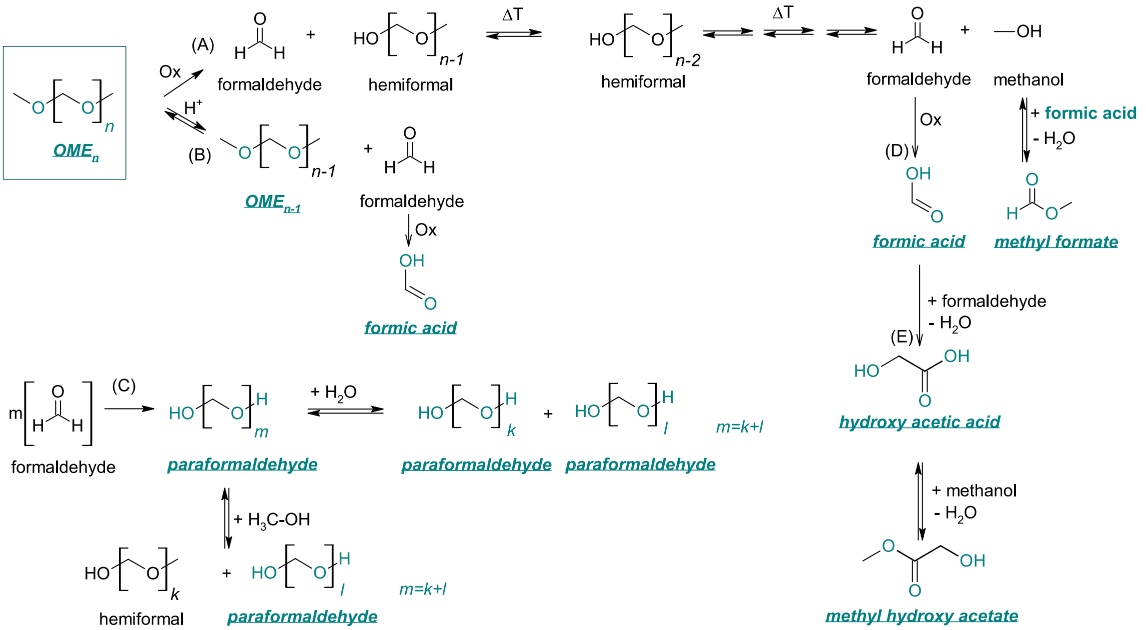

Fig. 5. Reaction pathway for the thermo-oxidative aging of OME, the compounds detected by GC–MS are highlighted. References used: (A): [20,45]; (B): [45]; (C): [17,63]; (D): [54,55]; (E): [60].

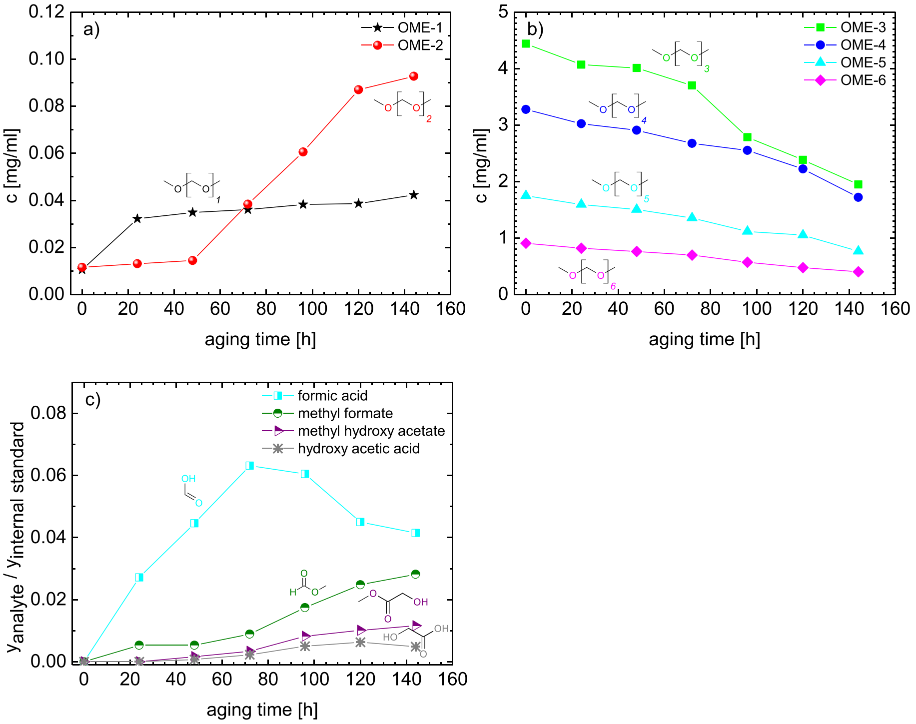

Fig. 6. a, b) Concentration as a function of the aging time of various products of the thermo-oxidative aging of oxymethylene ether (OME). c) Normalized peak area as a function of the aging time of various products of the thermo-oxidative aging of OME.

dimethyl-1,3-dioxolane-4-methanol-acetate.

To evaluate the time dependency of the solketal aging process, the concentration or the normalized peak areas of selected decomposition products were plotted over time (Fig. 4). The concentration of solketal and its isomer, hereinafter referred to as solketal, decreased exponentially from initially c = 10.26 mg/ml to a value of c = 5.23 mg/ml after 144 h i.e., ~ 49 % of the original concentration. The hydrolysis products glycerol and acetone were first detected after 24 h (first sample) with concentrations of c = 0.36 mg/ml and c = 0.32 mg/ml, respectively. The concentration of glycerol increased steadily from 24 h to 144 h up to a value of c = 3.41 mg/ml. In contrast, the concentration of acetone reached a plateau at 0.96 mg/ml after 96 h. The reason for the lower amount of acetone detected is suspected due to its high vapor pressure ($p_{v,\ acetone}$ (110 °C) = 4.78 bar) [62] leading to loss of acetone during sampling.

2,2-dimethyl-1,3-dioxolane-carboxaldehyde was also detected after 24 h aging with a concentration of c = 0.084 mg/ml. Interestingly, its concentration decreased steadily until it reached c = 0.0107 mg/ml after

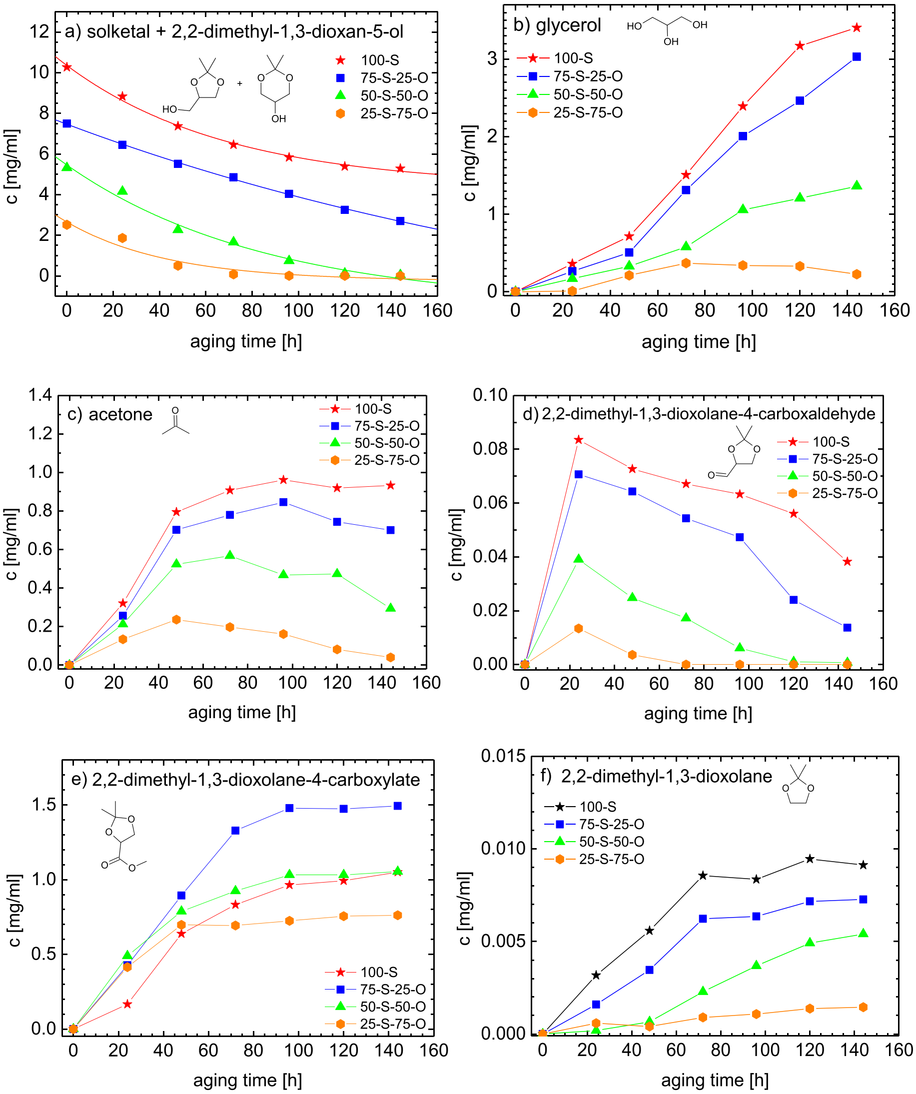

Fig. 7. a-f) Concentration of various products of the thermo-oxidative aging of mixtures of solketal and oxymethylene ether (OME) as a function of the aging time. 100-S: pure solketal, 100-O: pure $OME_{1\text{-}6}$, mixtures of 3:1 (75-S-25-O), 1:1 (50-S-50-O) and 1:3 (25-S-75-O) solketal:OME (vol%).

144 h. The most likely reason for this behavior are subsequent reactions, such as the oxidation to solketalic acid, proceeding at a faster rate than the formation of the aldehyde. Solketalic acid in turn forms 2,2-dimethyl-1,3-dioxolane via decarboxylation, which was detected with a concentration of c = 0.0032 mg/ml after 24 h of aging. The concentration of this product increased steadily and reached a plateau of ~ c = 0.0092 mg/ml after ~ 120 h of aging time. Furthermore, acetic acid and 2,2-dimethyl-1,3-dioxolane-methanol acetate were detected after 24 h. The concentration of both steadily increased until the end of the experiment. The presence of these compounds confirms the oxidative C–C bond cleavage of glycerol resulting in formaldehyde and acetaldehyde, with subsequent oxidation to acetic acid followed by esterification with solketal. The detection of 2-dimethyl-1,3-dioxolane-carboxylate after 24 h aging time with c = 0.17 mg/ml further confirms this reaction pathway, because it is formed by esterification of solketal and formic acid, which is an oxidation product of formaldehyde. The concentration of this ester increased steadily and reached a plateau after ~ 120 h with a maximum concentration of c = 1.05 mg/ml. Although they were not detected in the 24 h sample, it's reasonable to assume that formaldehyde and formic acid were already formed after 24 h aging due to the detection of 2-dimethyl-1,3-dioxolane-carboxylate.

The oxidation product of glycerol, glyceraldehyde, was first detected after 24 h. Its concentration increased steadily until the end of the experiment, indicating that it is not rapidly consumed by subsequent reactions. In addition to the previously detected molecules, acetine, the esterification product of glycerol and acetic acid, was first detected in the sample after 48 h, after which its concentration increased continuously. Hydroxy acetic acid and methyl hydroxy acetate, were both first detected after 96 h aging time, afterwards their concentration also increased until the end of the experiment. (1,3-dioxolane-4-yl)methanol and its isomer were also detected from 96 h onwards and showed an increasing concentration from initially c = 0.00645 mg/ml up to c = 0.0380 mg/ml at the end of the experiment. The reason for the late detection of hydroxy acetic acid, methyl hydroxy acetate, and (1,3-dioxolane-4-yl)methanol is suspected to be that the esterification to 2-dimethyl-1,3-dioxolane-carboxylate is highly favored in comparison to the reaction of glycerol or acetic acid with formaldehyde (Figs. 3 and 4 a-d). Overall, the detected products and the curve of their concentrations confirm the proposed reaction pathway.

In summary, the results of this experiment show that solketal is not stable against thermo-oxidative aging. After an aging time of 144 h, the initial concentration of solketal decreased by ~ 50 % and several products were formed mainly through hydrolysis, but also via oxidation, including oxidative C–C bond cleavage, followed by esterification. The main products formed during aging are glycerol, acetone, and 2-dimethyl-1,3-dioxolane-carboxylate.

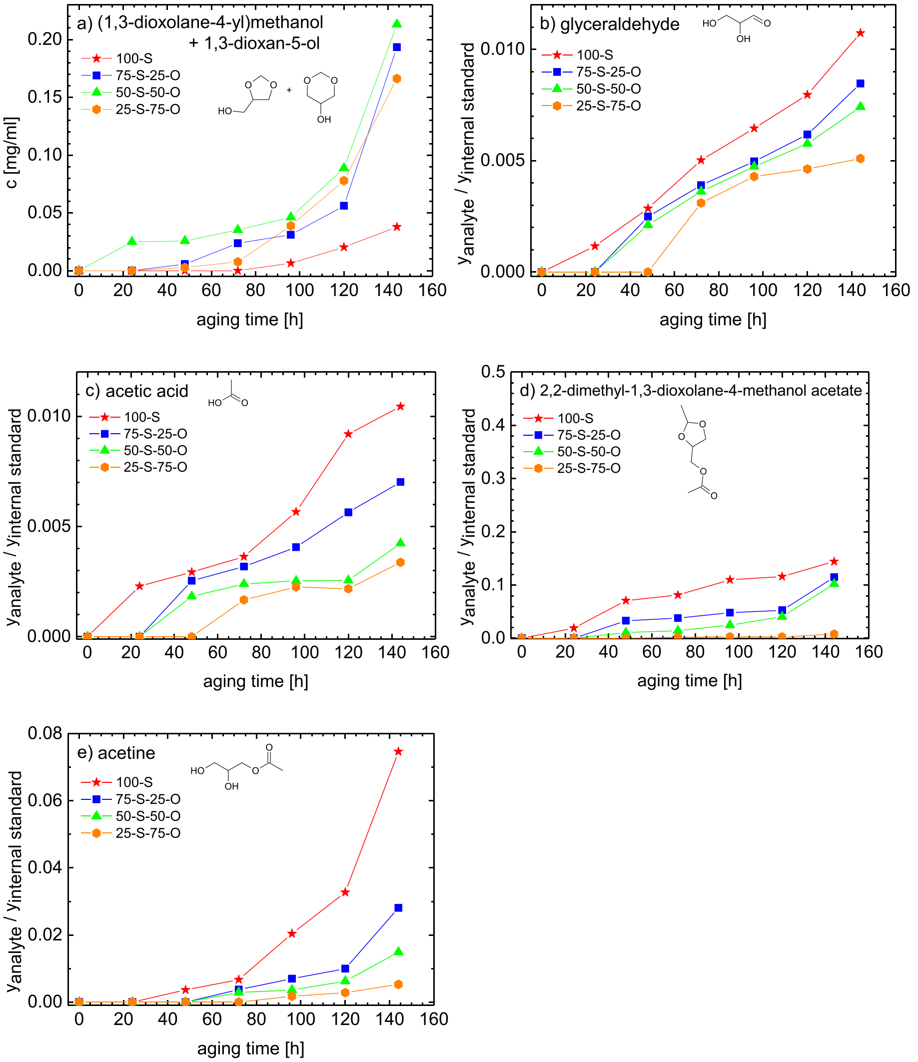

Fig. 8. a) Concentration of various products of the thermo-oxidative aging of mixtures of solketal and oxymethylene ether (OME) as a function of the aging time. b-e) Normalized peak area of various products of the thermo-oxidative aging of mixtures of solketal and OME as a function of the aging time. 100-S: pure solketal, 100-O: pure $OME_{1\text{-}6}$, mixtures of 3:1 (75-S-25-O), 1:1 (50-S-50-O) and 1:3 (25-S-75-O) solketal:OME (vol%).

3.2. Thermo-oxidative aging of OME

After solketal, OME was studied in a similar fashion. The specific sample of OME used in our study, contained a mixture of $OME_{1\text{-}6}$: 0.05 wt% OME_1, 0.06 wt% OME_2, 45.39 wt% OME_3, 5.11 wt% OME_3-derivative 25.39 wt% OME_4, 2.23 wt% OME_4-derivative (Fig. S1), 11.22 wt% OME_5 and 4.57 wt% OME_6[49]. In this study, this mixture is referred to as OME. During the aging process of OME, formic acid, methyl formate, hydroxy acetic acid, methyl hydroxy acetate, and paraformaldehyde were identified as aging products after different aging times (Table 3, Figure S3).

Based on these aging products and known reaction pathways from literature [17,20,45,55,60,63], the following reaction pathway for the thermo-oxidative aging of OME is postulated:

Formic acid and methyl formate (formed by esterification of formic acid and methanol), indicate degradation of OME_n to OME_{n-1}, releasing one equivalent of formaldehyde each step, until OME_1 decomposes to formaldehyde and methanol. This occurs either acid-catalyzed, resulting in a reduction of the chain-length of OME_n and the formation of formaldehyde [45] or through autoxidation resulting in the formation of formaldehyde and hemiformals [20,45]. Formic acid is then formed via oxidation of formaldehyde [54,55], and subsequently esterified with methanol to methyl formate. Formic acid can also react with formaldehyde, forming hydroxy acetic acid via C–C bond formation [60], which in turn can be esterified with methanol to form methyl hydroxy acetate. Formaldehyde can polymerize to paraformaldehyde at normal pressure and temperatures below 150 °C without the need of a catalyst usually reaching chain lengths m of $m = 8$–100 monomers. The presence of water results in shorter chains, due to hydrolysis [17,63]. Similarly, paraformaldehyde can react with methanol to form short-chain paraformaldehyde molecules and hemiformals [17]. The decomposition of paraformaldehyde to formaldehyde only takes place at temperatures above T = 150 °C [17]. An overview of this reaction network is shown in Fig. 5, whereby the compounds detected by GC–MS and FT-IR (in case of paraformaldehyde) are highlighted.

To evaluate the time dependency of the OME aging process, the concentration (or the normalized peak areas, respectively) of selected decomposition products were plotted over time (Fig. 6). After 24 h a substantial decrease of the concentration of $OME_{3\text{-}6}$ was observed. OME_3 and OME_4 decreased by ~ 8 %, OME_5 by ~ 9 %, and OME_6 by ~ 10 %. This decrease continued until the end of the experiment after 144 h. In the final sample, the concentration of OME_3 decreased by ~ 56 %, of OME_4 by ~ 47 %, of OME_5 by ~ 57 %, and of OME_6 by ~ 64 %, compared to the initial value. In contrast, the concentration of $OME_{1\text{-}2}$ was found to have increased after 24 h, for OME_2 by ~ 2 %, and for OME_1 by ~ 51 %. After 144 h of aging time the concentration of OME_2

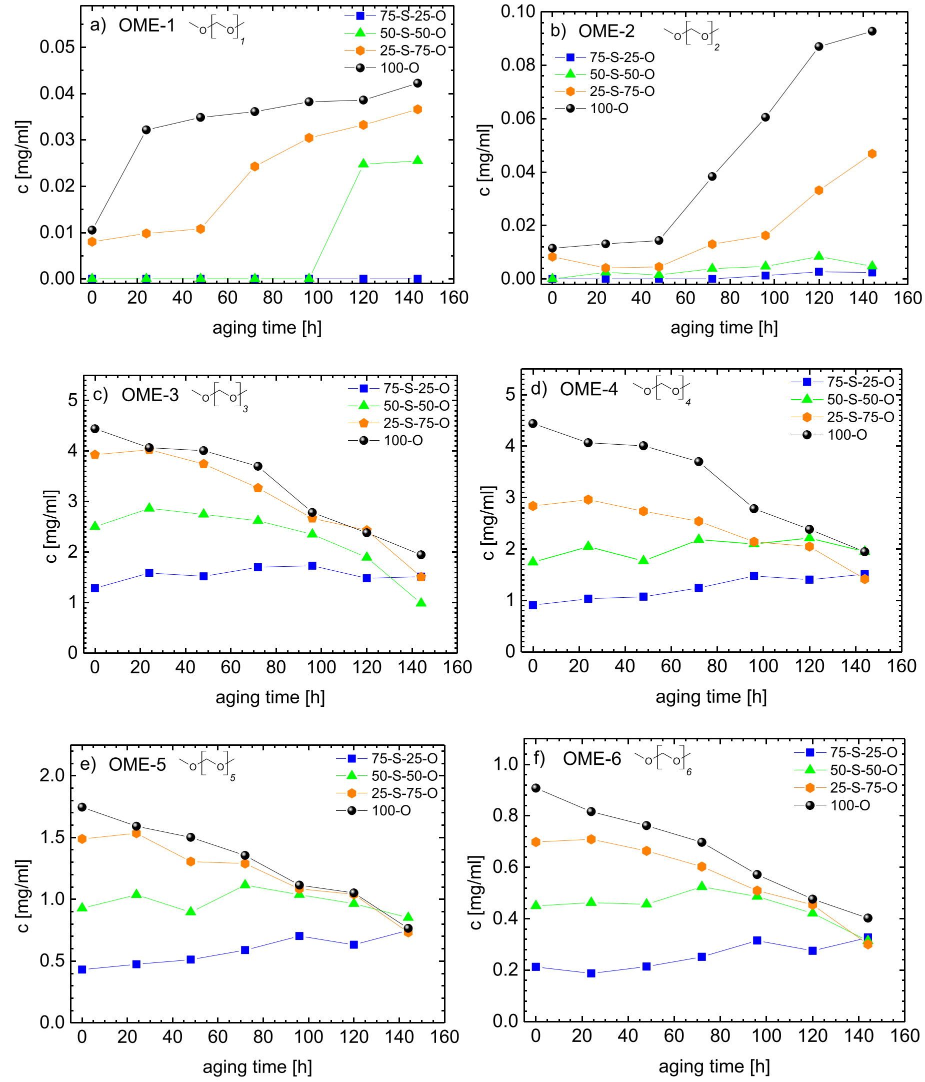

Fig. 9. a-f) Concentration of various products of the thermo-oxidative aging of mixtures of solketal and oxymethylene ether (OME) as a function of the aging time. 100-S: pure solketal, 100-O: pure OME_{1-6}, mixtures of 3:1 (75-S-25-O), 1:1 (50-S-50-O) and 1:3 (25-S-75-O) solketal:OME (vol%).

had increased to ~ 88 %, and to ~ 75 % for OME_1, respectively. The obvious explanation for this is the aforementioned degradation of OME chains, producing formaldehyde and shorter chain OME. Formaldehyde was not directly observed, but its oxidation product, formic acid, was first found after 24 h after which its concentration increased steadily until 72 h of aging time. From the 72-hour sample until the final sample at 144 h a decrease of formic acid concentration was detected. The reason for this behavior is probably the increased rate of subsequent reactions with other decomposition products after longer aging times. This can also be seen in the increasing concentrations of hydroxy acetic acid (first observed after 48 h aging), as well as the esters methyl formate and methyl hydroxy acetate, which both steadily increased from 24 h to 144 h aging.

From 72 h aging onwards, the formation of paraformaldehyde as a precipitate (colorless powder) in the three-neck flask and in the reflux condenser of the aging setup was observed. The amount of precipitate visually increased until the end of the experiment. However, since it was not possible to recover the precipitate quantitatively from the aging setup, exact numbers are not available. In summary, the investigation shows that OME_n is also not stable against thermo-oxidative aging. After an aging time of 144 h, the concentration of OME_{3-6} decreased by ~ 47 – 57 % of the initial value, while the concentration of the short-chain OME_{1-2} increased by about 2–51 % Additionally, paraformaldehyde precipitated as a colorless solid, which is a significant problem for application.

3.3. *Thermo-oxidative aging of mixtures of solketal and OME*

After investigating solketal and OME separately, the aging of solketal-OME-mixtures with solketal:OME ratios of: 3:1 (vol%) (75-S-25-O), 1:1 (vol%) (50-S-50-O) and 1:3 (vol%) (25-S-75-O) was also investigated. The initial samples of all mixtures contained solketal and its isomer, as well as OME_{3-6} and presumably OME_{1-2} in concentrations corresponding to the dilution with solketal. However, OME_{1-2} could not be detected in the 75-S-25-O and the 50-S-50-O sample, because their concentration was below the detection limit. During the aging process of all mixtures, a combination of the same aging products as for the individual components was observed. Therefore, it is concluded that the postulated reaction pathways for the aging of solketal and OME (Figs. 3 and 5) are also valid for the aging process of their mixtures. Nevertheless, the formation of the aging products over time differs significantly from the pure components (Figs. 7-10, Table S1).

The initial concentration of solketal and its isomer decreased from 24 h – 144 h for all mixtures, by ~ 64 % for 75-S-25-O, by ~ 95 % and by ~ 99 % for 25-S-75-O, respectively. The concentration of glycerol increased from 24 h - 144 h for 75-S-25-O and 50-S-50-O, but for 25-S-

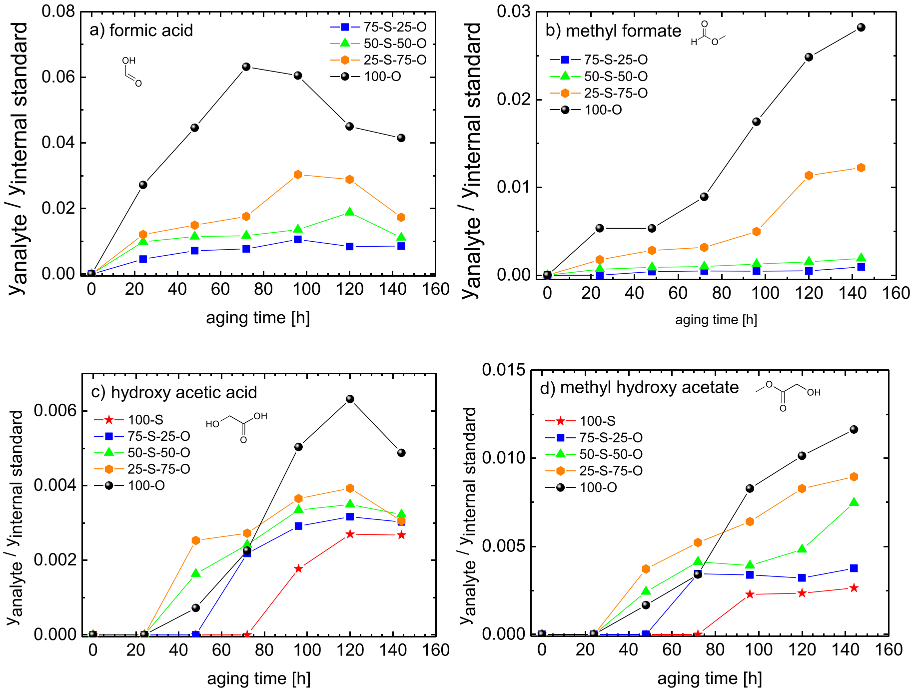

Fig. 10. a-d) Normalized peak area of various products of the thermo-oxidative aging of mixtures of solketal and OME as a function of the aging time. 100-S: pure solketal, 100-O: pure OME$_{1\text{-}6}$, mixtures of 3:1 (75-S-25-O), 1:1 (50-S-50-O) and 1:3 (25-S-75-O) solketal:OME (vol%).

Table 4

Fuel specific parameters (maximum values) of the thermo-oxidative aging of mixtures of solketal and oxymethylene ether (OME). 100-S: pure solketal, 100-O: pure OME$_{1\text{-}6}$, mixtures of 3:1 (75-S-25-O), 1:1 (50-S-50-O) and 1:3 (25-S-75-O) solketal:OME (vol%).

blend	total acid number (max. value) [mg KOH/g]	kin. viscosity [T = 40 °C] (max. value) [mm^2/s]	density [T = 15 °C] (max. value) [kg/m^3]
100-S	17.5	25.6	1.17
75-S-25-O	28.4	23.7	1.20
50-S-50-O	42.2	16.1	1.26
25-S-75-O	68.4	8.16	1.18
100-O	98.5	2.99	1.11

75-O the curve shows a maximum at 72 h (Fig. 7 b). Possibly, this is due to the formation of (1,3-dioxolane-4-yl)methanol, which was formed significantly more in mixtures with more OME (Fig. 8 a). This required glycerol and formaldehyde. For 25-S-75-O, the concentration of (1,3-dioxolane-4-yl)methanol increased from 24 h – 144 h, but at some point, not enough remaining solketal was available to reproduce glycerol. Therefore, the concentration of glycerol decreased again after 72 h of aging. The acetone concentration increased during aging and the curve shows a maximum at 96 h for 75-S-25-O, at 72 h for 50-S-50-O and a maximum at 48 h for 25-S-75-O (Fig. 7 c). The decrease at later aging times is possibly caused by increased evaporation of acetone in the open aging setup. The concentration of 2,2-dimethyl-1,3-dioxolane-4-carboxaldehyde (Fig. 7 d) as well as the concentration of 2,2-dimethyl-1,3-dioxolane (Fig. 7 f) show a similar progression for all mixtures with a maximum at 24 h. The concentration of 2,2-dimethyl-1,3-dioxolane-4-carboxylate (Fig. 7 e) increased steadily over the aging time of all mixtures and had the highest value for 75-S-25-O, followed by 50-S-50-O. The more solketal was present in the mixture, the more esterification to 2,2-dimethyl-1,3-dioxolane-4-carboxylate appeared.

The results also show that during aging of the OME-rich mixtures, more formic acid (Fig. 10 a) was produced and therefore more esterification to methyl formate (Fig. 10 b) occurred. Also, more hydroxy acetic acid and methyl hydroxy acetate were formed (Fig. 10 c, d). In contrast, the solketal-rich blends produced more glyceraldehyde, acetic acid, 2,2-dimethyl-1,3-dioxolane-4-methanol acetate and acetine (Fig. 8 b-e). The initial concentration of OME$_3$ (Fig. 9 c) decreased for all mixtures, while OME$_{4\text{-}6}$ (Fig. 9 d-f) decreased for 25-S-75-O but showed a higher stability towards aging in 75-S-25-O and 50-S-50-O. The OME$_5$ and OME$_6$ increased slightly for 75-S-25-O. The acid catalyzed degradation reaction of OME$_n$ to OME$_{n\text{-}1}$ (Fig. 5) can take place in both directions. Therefore, possibly OME$_{n\text{-}1}$ and formaldehyde could form OME$_n$. The OME$_2$ (Fig. 9 b) increased stronger for 25-S-75-O, only slightly for 50-S-50-O and almost not at all for 75-S-25-O. The OME$_1$ (Fig. 9 a) increased for all mixtures, except for 75-S-25-O. After 120 h paraformaldehyde has formed in 25-S-75-O and 50-S-50-O, but no precipitate formation was observed in the case of 75-S-25-O. The formation of paraformaldehyde depends on the methanol/formaldehyde ratio. If the methanol/formaldehyde ratio is > 0.5, no paraformaldehyde is formed [17]. This suggests that more formaldehyde compared to methanol formed during aging for 50-S-50-O and 25-S-75-O, but not for 75-S-25-O. The reason for this is possibly that there was a subsequent reaction of formaldehyde with solketal or its degradation products, e.g., the reaction of OME$_{n\text{-}1}$ and formaldehyde to OME$_n$. The formation of paraformaldehyde was suppressed by a higher concentration of solketal.

This study shows that the mixtures of solketal and OME are more stable against thermo-oxidative aging than the pure fuel components. This shows the potential strategy to increase stability through blending. The initial concentration of solketal decreased ~ by 64 % for 75-S-25-O, by ~ 95 % for 50-S-50-O and by ~ 99 % for 25-S-75-O. All products observed in the aging of the mixtures were also observed in the aging of the respective pure components. However, the concentration and aging time at which the products were formed varied depending on the composition of the mixture. The initial concentration of OME$_n$ with n >= 3 decreased, while the concentration of OME$_1$ increased for all mixtures, indicating chain degradation. However, a higher stability of OME$_n$ n > 3 was observed in 75-S-50-O and 50-S-50-O. Additionally, the

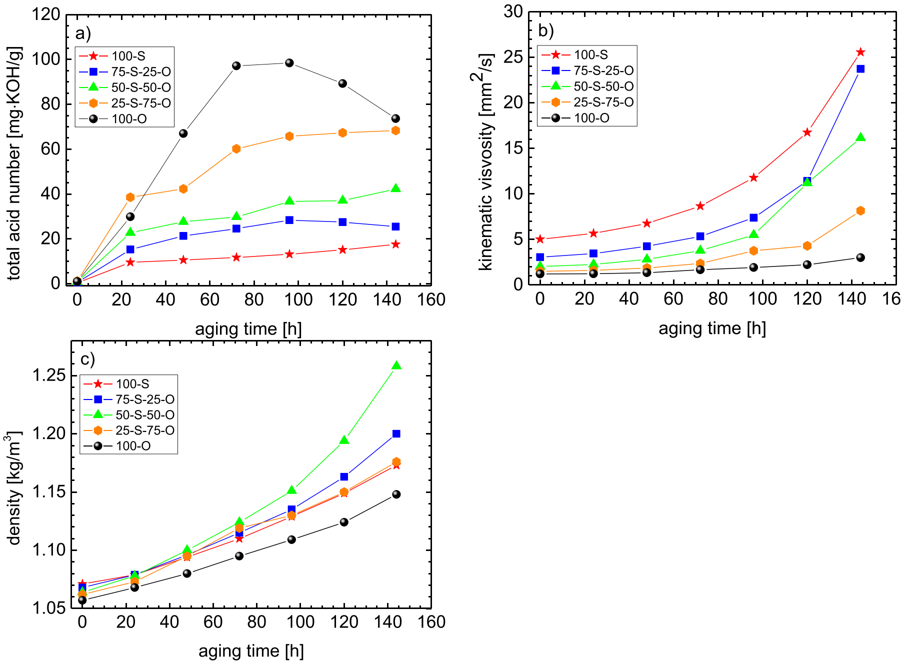

Fig. 11. a) Total acid number as a function of the aging time of solketal, oxymethylene ether (OME) and mixtures of solketal and OME. b) Kinematic viscosity as a function of the aging time of solketal, OME and mixtures of solketal and OME. c) Density as a function of the aging time of solketal, OME and mixtures of solketal and OME. 100-S: pure solketal, 100-O: pure $OME_{1\text{-}6}$, mixtures of 3:1 (75-S-25-O), 1:1 (50-S-50-O) and 1:3 (25-S-75-O) solketal:OME (vol%).

formation of paraformaldehyde as a precipitate was observed in 25-S-75-O and 50-S-50-O, but not in 75-S-25-O. The formation of precipitates during aging is particularly problematic in the use of fuels because they can cause severe damage to combustion engines. In summary, 75-S-25-O is the most promising mixture in terms of stability to thermo-oxidative aging. Due to its higher stability, it could be a good candidate for further optimization in a ternary fuel blend.

3.4. *Determination of fuel specific parameters*

The viscosity and density of a fuel are two parameters that can influence engine performance and emissions. Moreover, the total acid number is an important parameter for the degree of aging, especially for e-fuels. TAN increased during aging of pure solketal, pure OME and all mixtures. In case of 100-O, the TAN showed the highest values of all aged fuels with a maximum value at 96 h ($TAN_{100\text{ - }O} = 98.5$ mg KOH/g). The obvious reason for this is the formation of formic acid. The formation of methyl formate could explain the decrease of the TAN, which is a measure of the content of free carboxylic acids that are not bound as esters, after 96 h aging. The TAN of pure solketal (100-S) and of all mixtures increased during aging and reached a plateau at ~ 96 h. The maximum values of the TAN of all blends are shown in Table 4.

The results show, that the TAN increased during aging for the pure fuels and all mixtures, the more OME was present in the mixture, the higher the TAN values due to formation of acids (Fig. 11, Table 4 and Table S2). This is problematic because acidic compounds in the fuel can lead to corrosion and engine wear. The kinematic viscosity increased during aging of pure solketal, pure OME, and all mixtures. The maximum values are shown in Table 4. Higher solketal content in the mixture, resulted in higher kinematic viscosity values after aging (Fig. 11 b and Table S2). It is speculated that the increase in viscosity during aging is a result of the formation of highly viscos glycerol from solketal during aging. However, the viscosity values of 75-S-25-O and 50-S-50-O were still in the range of the fuel standard DIN EN590 up to ~ 72 h aging.

The density of 100-S, 100-O and all mixtures also increased during aging (Fig. 11 c, Table 4, Table S2). This is due to the formation of several aging products in varying concentration. The density of the aged 50-S-50-O showed the highest values of all mixtures. This indicates a good intramolecular interaction and miscibility of the molecules.

In total, the fuel specific parameters indicate that the mixtures, especially 75-S-25-O could be used for a ternary blend, for example, with a fraction of 33 % like in the fuel Diesel R33 [31]: 25 vol% solketal and 8 vol% OME could be mixed with 67 vol% conventional diesel fuel. Alternatively, the 75-S-25-O could also be mixed with FAME or HVO to produce a completely regenerative fuel. However, further investigations of the combustion properties and miscibility is required before these fuels can be used.

4. Conclusions

The thermo-oxidative aging of the two promising e-fuels solketal and oxymethylene ether (OME_1 – OME_6) in pure form as well as in mixtures with different ratios (3:1, 1:1, and 1:3) (vol%) was investigated. Both reaction pathways of the thermo-oxidative aging process as well as the concentrations of the formed aging products as a function of the aging time were elucidated in detail. Furthermore, fuel-specific parameters such as the total acid number, the kinematic viscosity and the density of the aged and unaged fuels have been analyzed.

By mixing solketal and OME in a 3:1 ratio (vol%), the formation of solid paraformaldehyde, which is a major problem, could be successfully suppressed. Nevertheless, significant degradation of the initial fuels during the accelerated thermo-oxidative aging was found, with significant formation of problematic aging products. To overcome these problems, the use of solketal and OME as components in ternary blends is suggested, similar to the fuel Diesel R33 [31] consisting of conventional diesel fuel, FAME or HVO. Alternatively, ternary mixtures of OME and solketal with FAME or other renewable fuels could produce a viable option for a purely sustainable fuel blend. Future studies should focus on these blends, i.e., further investigations should be carried out regarding combustion properties and the influence of additives such as antioxidants and stabilizers to pave the way for future e-fuels that can be used on the market.

CRediT authorship contribution statement

Anne Lichtinger: Writing – review & editing, Supervision. **Maximilian J. Poller:** Writing – review & editing, Supervision. **Olaf Schröder:** Writing – review & editing, Supervision. **Julian Türck:** Writing – review & editing, Supervision. **Thomas Garbe:** Writing – review & editing, Supervision. **Jürgen Krahl:** Writing – review & editing, Supervision. **Markus Jakob:** Writing – review & editing, Supervision. **Jakob Albert:** Writing – review & editing, Supervision.

Declaration of competing interest

The authors declare that they have no known competing financial interests or personal relationships that could have appeared to influence the work reported in this paper.

Acknowledgements

We thank the Forschungsvereinigung Verbrennungskraftmaschinen e.V. (FVV 601342) and the Oberfrankenstiftung (FP00067) for the financial support of the research. Additionally, we thank the chairman of the project Dr. Bernd Becker and ASG for providing the different OME_n.

Appendix A. Supplementary data

Supplementary data to this article can be found online at https://doi.org/10.1016/j.fuel.2025.134738.

Data availability

Data will be made available on request.

References

[1] Pütz R. European Policy on Future Road Mobility - Technology right of way or headed in the wrong direction? *MVM* 2022;48(2):1–18.
[2] Lichtinger A, Poller MJ, Türck J, Schröder O, Garbe T, Krahl J, et al. Nile Red as a Fluorescence Marker and Antioxidant for Regenerative Fuels. *Energy Tech* 2023;11(11).
[3] Türck J, Schmitt F, Anthofer L, Lichtinger A, Türck R, Ruck W, et al. Oxidation Kinetics of Neat Methyl Oleate and as a Blend with Solketal. *Energies* 2023;16(7):3253.
[4] Nanda MR, Zhang Y, Yuan Z, Qin W, Ghaziaskar HS, Xu C. Catalytic conversion of glycerol for sustainable production of solketal as a fuel additive: A review. *Renew Sustain Energy Rev* 2016;56:1022–31.
[5] Mayank R, Ranjan A, Moholkar VS. Mathematical models of ABE fermentation: review and analysis. *Crit Rev Biotechnol* 2013;33(4):419–47.
[6] Türck J, Singer A, Lichtinger A, Almaddad M, Türck R, Jakob M, et al. Solketal as a renewable fuel component in ternary blends with biodiesel and diesel fuel or HVO and the impact on physical and chemical properties. *Fuel* 2022;310:122463.
[7] Malaya Ranjan Nanda (2015) Catalytic Conversion of Glycerol to Value-Added Chemical Products, Dissertation.
[8] Li L, Korányi TI, Sels BF, Pescarmona PP. Highly-efficient conversion of glycerol to solketal over heterogeneous Lewis acid catalysts. *Green Chem*, 2012;14(6):1611.
[9] Nanda MR, Yuan Z, Qin W, Ghaziaskar HS, Poirier M-A, Xu CC. Thermodynamic and kinetic studies of a catalytic process to convert glycerol into solketal as an oxygenated fuel additive. *Fuel* 2014;117:470–7.
[10] Vol'eva, V.B., Belostotskaya, I.S., Malkova, A.V., Komissarova, N.L., Kurkovskaya, L.N., Usachev, S.V., Makarov, G.G. (2012) New approach to the synthesis of 1,3-dioxolanes. *Russ J Org Chem*, **48** (5), 638–641.
[11] Manjunathan P, Maradur SP, Halgeri AB, Shanbhag GV. Room temperature synthesis of solketal from acetalization of glycerol with acetone: Effect of crystallite size and the role of acidity of beta zeolite. *J Mol Catal A Chem* 2015;396:47–54.
[12] Maksimov AL, Nekhaev AI, Ramazanov DN, Arinicheva YA, Dzyubenko AA, Khadzhiev SN. Preparation of high-octane oxygenate fuel components from plant-derived polyols. *Pet Chem*, 2011;51(1):61–9.
[13] Foster AB, Randall MH, Webber JM. Aspects of Stereochemistry, Reaction of 3-O. Methyl-D-glucitol with Acetone and Benzaldehyde. *Chemistry Department, The University, Edgbaston, Birmingham* 1965;15:3388–94.
[14] Samoilov VO, Borisov RS, Stolonogova TI, Zarezin DP, Maximov AL, Bermeshev MV, et al. Glycerol to renewable fuel oxygenates. Part II: Gasoline-blending characteristics of glycerol and glycol derivatives with C3-C4 alkyl(idene) substituents. *Fuel* 2020;280:118585.
[15] Pariente S, Tanchoux N, Fajula F. Etherification of glycerol with ethanol over solid acid catalysts. *Green Chem*, 2009;11(8):1256.
[16] Mota CJA, Da Silva CXA, Rosenbach N, Costa J, Da Silva F. Glycerin Derivatives as Fuel Additives: The Addition of Glycerol/Acetone Ketal (Solketal) in Gasolines. *Energy Fuels* 2010;24(4):2733–6.
[17] Oestreich, D. (2017) Prozessentwicklung zur Gewinnung von Oxymethylenethern (OME) aus Methanol und Formaldehyd, Dissertation. *KIT Scientific Publishing.*
[18] Gelner, A.D. (2022) OME als Wegbereiter klimaneutraler und schadstofffreier Dieselmotoren, Dissertation. *TUM School of Engineeing and Design.*
[19] Staudinger H, Signer R, Johner H, Lüthy M, Kern W, Russidis D, et al. Über hochpolymere Verbindungen. Über die Konstitution der Polyoxymethylene. *Justus-Liebigs Annalen der Chemie* 1929;1:145–275.
[20] Bogatykh I, Osterland T, Stein H, Wilharm T. Investigation of the Oxidative Degradation of the Synthetic Fuel Oxymethylene Dimethyl Ether. *Energy Fuels* 2020;34(3):3357–66.
[21] Burger J, Siegert M, Ströfer E, Hasse H. Poly(oxymethylene) dimethyl ethers as components of tailored diesel fuel: Properties, synthesis and purification concepts. *Fuel* 2010;89(11):3315–9.
[22] Burger J, Ströfer E, Hasse H. Chemical Equilibrium and Reaction Kinetics of the Heterogeneously Catalyzed Formation of Poly(oxymethylene) Dimethyl Ethers from Methylal and Trioxane. *Ind Eng Chem Res*, 2012;51(39):12751–61.
[23] Burger J, Ströfer E, Hasse H. Production process for diesel fuel components poly (oxymethylene) dimethyl ethers from methane-based products by hierarchical optimization with varying model depth. *Chem Eng Res Des* 2013;91(12):2648–62.
[24] Schmitz N, Ströfer E, Burger J, Hasse H. Conceptual Design of a Novel Process for the Production of Poly(oxymethylene) Dimethyl Ethers from Formaldehyde and Methanol. *Ind Eng Chem Res*, 2017;56(40):11519–30.
[25] Wesner A, Kampe P, Herrmann N, Eller S, Ruhmlieb C, Albert J. Indium-based Catalysts for CO 2 Hydrogenation to Methanol: Key Aspects for Catalytic Performance. *ChemCatChem* 2023;15(24).
[26] Reuss, G., Disteldorf, W., Gamer, A.O., Hilt, A. (2000) Formaldehyde, in *Ullmann's Encyclopedia of Industrial Chemistry*, Wiley-VCH Verlag GmbH & Co. KGaA, Weinheim, Germany.
[27] Ren Y, Huang Z, Miao H, Di Y, Jiang D, Zeng K, et al. Combustion and emissions of a DI diesel engine fuelled with diesel-oxygenate blends. *Fuel* 2008;87(12):2691–7.
[28] Ras K, Kusenberg M, Vanhove G, Fenard Y, Eschenbacher A, Varghese RJ, et al. A detailed experimental and kinetic modeling study on pyrolysis and oxidation of oxymethylene ether-2 (OME-2). *Combust Flame* 2022;238:111914.
[29] DIN EN 590 (2019).
[30] Alptekin E, Canakci M. Performance and emission characteristics of solketal-gasoline fuel blend in a vehicle with spark ignition engine. *Appl Therm Eng* 2017;124:504–9.
[31] Götz, K., Fey, B., Singer, A., Krahl, J., Bünger, J., Knorr, M., Schröder, O. (2016) Exhaust Gas Emissions and Engine Oil Interactions from a New Biobased Fuel Named Diesel R33, in *SAE Technical Paper Series*. SAE 2016 International Powertrains, Fuels & Lubricants Meeting, OCT. 24, 2016. SAE International400 Commonwealth Drive, Warrendale, PA, United States.
[32] Pradelle F, Braga SL, Martins ARFA, Turkovics F, Pradelle RNC. Gum Formation in Gasoline and Its Blends: A Review. *Energy Fuels* 2015;29(12):7753–70.
[33] Rizwanul Fattah IM, Masjuki HH, Kalam MA, Hazrat MA, Masum BM, Imtenan S, et al. Effect of antioxidants on oxidation stability of biodiesel derived from vegetable and animal based feedstocks. *Renew Sustain Energy Rev* 2014;30:356–70.
[34] Pereira, R.C.C. and Pasa, V.M.D. (2006) Effect of mono-olefins and diolefins on the stability of automotive gasoline. *Fuel*, **85** (12-13), 1860–1865.
[35] B D Batts and Zuhdan Fathoni - A Literature Review on Fuel.
[36] Sharma YK. The Instability of Storage of Middle Distillate Fuels: A Review. *Pet Sci Technol* 2012;30(17):1839–50.
[37] Rizwanul Fattah IM, Masjuki HH, Kalam MA, Mofijur M, Abedin MJ. Effect of antioxidant on the performance and emission characteristics of a diesel engine fueled with palm biodiesel blends. *Energ Conver Manage* 2014;79:265–72.
[38] Botella L, Bimbela F, Martín L, Arauzo J, Sánchez JL. Oxidation stability of biodiesel fuels and blends using the Rancimat and PetroOXY methods. Effect of 4-allyl-2,6-dimethoxyphenol and catechol as biodiesel additives on oxidation stability. *Front Chem* 2014;2:43.
[39] Flitsch S, Neu PM, Schober S, Kienzl N, Ullmann J, Mittelbach M. Quantitation of Aging Products Formed in Biodiesel during the Rancimat Accelerated Oxidation Test. *Energy Fuels* 2014;28(9):5849–56.
[40] Cychy S, Lechler S, Muhler M. Selective Anodic Oxidation of Solketal as Acetal-Protected Glycerol over Nickel Boride in Alkaline Media to Glyceric Acid**. *ChemElectroChem* 2022;9(4).
[41] Kumari B, Braun M, Cychy S, Sanjuán I, Behrendt G, Behrens M, et al. Electrooxidation of the Glycerol Derivative Solketal over Cu−Co Hydroxycarbonates to Enable the Synthesis of Glyceric Acid. *ChemElectroChem* 2023;10(8).
[42] Moity L, Benazzouz A, Molinier V, Nardello-Rataj V, Elmkaddem MK, de Caro P, et al. Glycerol acetals and ketals as bio-based solvents: positioning in Hansen and COSMO-RS spaces, volatility and stability towards hydrolysis and autoxidation. *Green Chem*, 2015;17(3):1779–92.
[43] Bacha K, Ben-Amara A, Vannier A, Alves-Fortunato M, Nardin M. Oxidation Stability of Diesel/Biodiesel Fuels Measured by a PetroOxy Device and Characterization of Oxidation Products. *Energy Fuels* 2015;29(7):4345–55.
[44] Türck J, Schmitt F, Anthofer L, Türck R, Ruck W, Krahl J. Extension of Biodiesel Aging Mechanism-the Role and Influence of Methyl Oleate and the Contribution of Alcohols Through the Use of Solketal. *ChemSusChem* 2023;16(17):e202300263.
[45] Cherdron H, Höhn L, Kern W. Der acidolytische abbau von polyoxymethylenen.: 18. Mitt. In: über Polyoxymethylene. Organisch-Chemisches Institut der Universität Mainz; 1962. p. 48–58.

[46] Blyumenfel'd AB, Neiman MB, Kovarskaya BM. Products of the thermo-oxidative degradation of Polyformaldehyde. *Polym Sci.* 1966;8:2199–206.
[47] Dudina KA, Berlin AA, Karmilova LV, Enikolopyan NS. Change of molecular weight in the oxidative destruction of polyformaldehyde. *Dokl Akad Nauk SSSR* 1963;150: 580–3.
[48] Sedlar VJ, Kucera M. Der thermooxydative Abbau von Polyformaldehyd. *Die Makromolekulare Chemie* 1967;102:245–58.
[49] ASG Analytik-Service AG (2021) Prüfbericht 2900573: ASG-ID 2900573_001.
[50] Lichtinger A, Poller MJ, Schröder O, Türck J, Garbe T, Krahl J, et al. (2024) Thermo-oxidative aging of linear and branched alcohols as stability criterion for their use as e-fuels. *Sustainable Energy Fuels* 2024;8:3329–40.
[51] DIN EN 14112 (2016).
[52] DIN EN 15751 (2008).
[53] Harold W. Gardner (1988) Oxygen radical chemistry of polyunsaturated fatty acids. *Free Radic Biol Med* 1989;7:65–86.
[54] Sheldon, R.A. and Kochi, J.K. (1981) Metal-Catalyzed Oxidations of Organic Compounds: Mechanistic Principles and Synthetic Methodology Including Biochemical Processes, Elsevier Science, New York, London, Toronto, Sydney, San Francisco.
[55] Larkin DR. The Role of Catalysts in the Air Oxidation of Aliphatic Aldehydes. *J Org Chem* 1990;55:1563–8.
[56] Sanwald KE, Berto TF, Eisenreich W, Gutiérrez OY, Lercher JA. Catalytic routes and oxidation mechanisms in photoreforming of polyols. *J Catal* 2016;344:806–16.
[57] Stein YS, Antal MJ. PII: 0165-2370(83)80003-5. *J Anal Appl Pyrol* 1983;4:283–96.
[58] Rashba-Step J, Step E, Turro NJ, Cederbaum AI. Rashba-Step_1994. *Biochemistry* 1994;33:9504–10.
[59] Ai M. PII: 0021-9517(87)90285-5. *J Catal* 1987;107:201–8.
[60] Morooka S, Wakai C, Matubayasi N, Nakahara M. Hydrothermal carbon-carbon bond formation and disproportionations of C1 aldehydes: formaldehyde and formic acid. *Chem A Eur J* 2005;109(29):6610–9.
[61] Martinuzzi I, Azizi Y, Devaux J-F, Tretjak S, Zahraa O, Leclerc J-P. Reaction mechanism for glycerol dehydration in the gas phase over a solid acid catalyst determined with on-line gas chromatography. *Chem Eng Sci* 2014;116:118–27.
[62] Ambrose D, Sprake CHS, Townsend R. Thermodynamic properties of organci oxygen compounds: XXXIII. The vapour pressure of acetone. *J Chem Thermodynamics* 1974;6:693–700.
[63] Salamanca JC, Munhenzva I, Escobedo JO, Jensen RP, Shaw A, Campbell R, et al. Formaldehyde Hemiacetal Sampling, Recovery, and Quantification from Electronic Cigarette Aerosols. *Sci Rep* 2017;7(1):11044.